Regular Article

PHYSICAL CHEMISTRY RESEARCH
Published by the
Iranian Chemical Society
www.physchemres.org
info@physchemres.org

***Phys. Chem. Res.**, Vol. 1, No. 2, 175-184, December 2013.*

Computational Study on the Energetic and Electronic Aspects of Tautomeric Equilibria in 5-Methylthio-1,2,4-triazole

T. Hosseinnejad

Department of Chemistry, Faculty of Science, Alzahra University, Vanak, Tehran, Iran

(Received 20 July 2013, Accepted 17 September2013)

The main purpose of this research is to investigate computationally the tautomeric reaction pathway of 5-methyl-3-methylthio-1,2,4-triazole from the thermodynamical and mechanistical viewpoints. In this respect, density functional theory (DFT) in conjunction with the quantum theory of atoms in molecule (QTAIM) has been employed to model the energetic and electronic features of tautomeric mechanism in the gas phase. Moreover, the effect of two different solvents, dimethylformamide (DMF) and H_2O, has been examined *via* the polarized continuum model (PCM) calculations. Then, we have presented the potential energy profile for the two-step tautomeric reaction in the gas and solution phases and analyzed comparatively the energetic aspects of tautomers, intermediate and transition states. Additionally, we have concentrated on the survey of tautomerism by means of topological electronic indices. Strictly speaking, QTAIM calculations have been performed to explore the variation of electronic density and its laplacian at some key bond critical points of tautomers, intermediate and transition states and also to interpret the proposed tautomeric mechanism.

Keywords: 1,2,4 Triazoles, Tautomeric reaction, Density functional theory, QTAIM analysis, Polarized continuum model

INTRODUCTION

Many compounds bearing five-membered rings such as triazoles constitute rich and important field in biological aspects [1,2]. They were shown to be effective as anti-inflammatory, antibacterial, anticonvulsant, dephlogisticate and antifungal agents and more importantly are building blocks for the nucleic bases [3-5]. These five-membered heterocycles possess two types of nitrogen atoms, namely pyrole-like and pyridine-like nitrogen atoms [6]. So, the presence of these two types of nitrogen atoms leads to the interchange of protons in the process of prototropic tautomerism [7,8].

Recently, experimental results related to the palladium-catalyzed regioselective hetero-cyclization of allylmercapto-1,2,4-triazoles to thiazolo-1,2,4-triazoles, show producing two regioisomeric final products. This regioselectivity can be mainly attributed to the relative stability of two tautomeric structures of 1,2,4-triazole species which affects significantly on the mode of intermolecular cyclization process and consequently the regioselectivity of final products [9-11].

In continuation of our previous work on computational investigation of the origin of regioselectivity in synthesis of 6-(4-nitrobenzyl)-2-phenylthiazolo[3,2-b]1,2,4-triazole [12], we have concentrated on the tautomeric reaction of 5-methyl-3-methylthio-1,2,4-triazole as an appropriate model for tautomerism of allylmercapto-1,2,4-triazoles, from the mechanistic and thermodynamic viewpoints. The aforesaid tautomeric reaction has been illustrated schematically in Fig.1.

Indeed, the important role of tautomeric reaction of thio-substituted 1,2,4-triazloes in regioselective synthesis of thiazolo-1,2,4-triazoles and also the encouraging biological activities of these compounds, are the major promotion for us in computational study of aforementioned tautomeric reaction. To the best of our knowledge, it does not exist any theoretical investigation on the tautomeric equilibria of 5-methyl-3-methylthio-1,2,4-triazole in the literature.

In this research, we have mainly focused on the survey of aforesaid proton-transfer reaction mechanistically and

*Corresponding authors. E-mail: tayebeh.hosseinnejad@alzahra.ac.ir

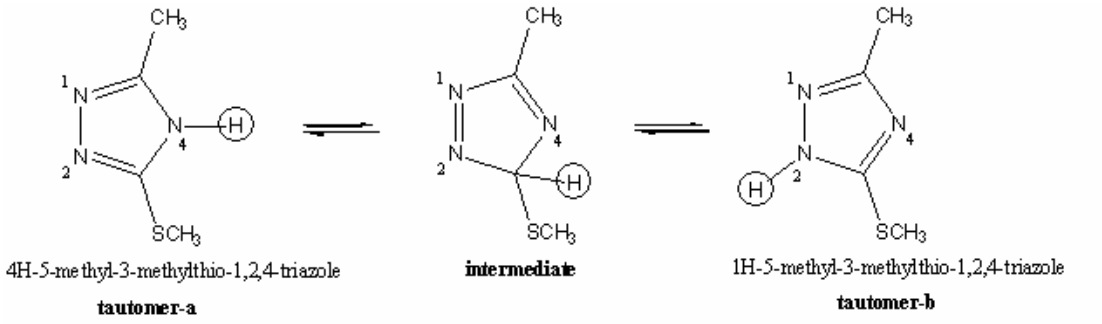

Fig. 1. Schematic diagram of tautomeric reaction investigated in this work, including chemical structures and their numbering.

thermodynamically by means of DFT methods using two functionals B3LYP/6-311+G** and M06/6-311+G** orbital basis sets [13-15]. In the next step, the effect of various chemical environments on the energetics of tautomerism has been analyzed comparatively from the mechanistical and thermodynamical viewpoints. However, the polarized continuum model (PCM) [16] was adopted to evaluate the electronic energies and thermodynamical properties of tautomers, intermediate and transition states. It should be noted that the preference of using polar and aprotic solvents has been assessed thermodynamically in our previous work [12] and various experimental studies [17,18].

It is worthwhile to mention that the obtained information about the mechanism of proton transfer can be examined through simultaneous analysis of the evolution of some key electronic properties along the reaction coordinate. In this respect, we have assessed the variation of some selected electronic features through tautomeric reaction pathway *via* QTAIM approach [19]. Strictly speaking, electron densities, ellipticity, the electronic kinetic and potential energy densities have been analyzed to interpret the obtained potential energy profile of the mechanism of tautomerization reaction.

COMPUTATIONAL DETAIL

The mechanistic study of aforementioned tautomeric reaction was carried out by determining optimized structures corresponding to the ground states and the transition states on the reaction energy hyper-surface.

All calculations were performed using GAMESS suite of programs [20] *via* DFT method, based on B3LYP [13,14] and M06 functionals [15] in connection with 6-311+G** orbital basis sets. It should be stated that the popular B3LYP functional consists of a hybrid Becke-Hartree-Fock exchange and a Lee-Yang-Parr correlation function with nonlocal corrections.M06 functional has been introduced recently as a hybrid meta-GGA (generalized gradient approximation) exchange-correlation functional that was parametrized including both transition metals and nonmetals and was recommended for application in organometallic and inorganometallic thermochemistry, kinetic studies and noncovalent interactions. Moreover, the harmonic frequency analysis was used to confirm that the found structures correspond either to minima (number of imaginary frequencies equals 0) or transition states (number of imaginary frequencies equals 1) and unscaled frequencies from vibrational analysis were also employed to obtain enthalpies and Gibbs free energies in the standard state (1 atm and 298.15 K). Additionally, intrinsic reaction coordinate (IRC) analysis was applied to verify that the obtained transition state connects reactants and products [21,22]. However, the effect of solvent on the mechanistic and thermodynamic features of tautomerism has been examined on the basis of a continuum representation of the solvent surrounding the substances *via* PCM method [16].

In the next stage, Bader's topological QTAIM analysis [19] has been employed to assess the variation of some

electronic features of key bonds along tautomeric reaction by performing AIM 2000 program package [23] at M06/6-311+G** level of theory. In this respect, we have evaluated electron density, $\rho(r)$, its laplacian, $\nabla^2\rho(r)$, ellipticity, ε, the electronic kinetic energy density, $G(r)$, the electronic potential energy density, $V(r)$, and the total electronic energy density, $H(r)$, of bond critical points (BCPs) to analyze the obtained mechanistic interpretations of tautomeric reaction.

RESULTS AND DISCUSSION

Tautomeric Reaction Pathway: Mechanistic and Thermodynamic Viewpoints

The first part of this article deals with the computational assessment of reaction pathway for the tautomeric equilibrium between two tautomers of 5-methyl-3-methylthio-1,2,4-triazole, namely **tautomer-a** and **tautomer-b** (as illustrated in Fig. 1). In this respect, we have firstly calculated the relative stability of two aforementioned tautomers by determining absolute electronic energies and thermochemical properties in the gas phase, corresponded to their optimized structures. The obtained M06/6-311+G** optimized geometries of tautomers, intermediate and their corresponding transition states are shown in Fig. 2. In Table 1, we present the difference of electronic energy values between **tautomer-a** and **tautomer-b**, as electronic energy changes ($\Delta E_{e,r}$), zero-point included electronic energy changes ($\Delta E_{0,r}$), enthalpy changes (ΔH_r) and Gibbs free energy changes (ΔG_r) calculated at B3LYP/6-311+G** and M06/6-311+G** levels of theory in the gas phase and also in the presence of two solvents, DMF and H_2O. As discussed earlier, the assessment of the reaction environment effect in estimation of the reaction energetic is a challenging task in theoretical calculations. Therefore, in the next step, we calculate the reaction energy and thermodynamic properties changes in the presence of two solvents, DMF and H_2O.

The following three facts can be revealed from the reported results in Table 1: i) the **tautomer-b** is more stable thermodynamically than **tautomer-a** in the gas and solution phases on the basis of two levels of theory calculations ii) The employment of M06 functional in calculation of electronic energy and thermodynamic properties changes leads to the more negative values in comparison with using B3LYP functional and iii) by a comparative survey in the calculated Gibbs free energy changes (ΔG_r) in the gas and solution phases, it can be deduced that thermodynamic feasibility of tautomerism decreases in the solution phases while B3LYP/6-311+G** and M06/6-311+G** calculated ΔG_r values increase from -5.9 and -10.3 kcal mol^{-1} in the gas phase to -3.4 and -4.9 kcal mol^{-1} in the solution medium, respectively. It is worthwhile to note that there is a little thermodynamical distinction between using two solvents, DMF and H_2O. Another important aspect that can be apprehended from the computed values of ΔG_r is that the thermodynamic feature of tautomeric reaction does not differ significantly from the calculated enthalpy changes, ΔH_r, that could be assigned to the weak entropic effect in the aforementioned tautomeric reaction.

In the next stage, we confine our attention on the tautomeric reaction pathway *via* DFT calculations on the basis of B3LYP and M06 functionals in connection with 6-311+G** orbital basis sets. The tautomerization process that we investigated in this study belongs to 1,3 proton transfer group and occurs in two consecutive steps. This two-step tautomerization pathway is initiated by breaking N4-H σ-bond in **tautomer-a** (M06/6-311+G** calculated bond distance is 1.010 Å) to form C3-H bond in the intermediate species (M06/6-311+G**calculated bond distance is 1.104 Å) with the subsequent transition state, **TS-a**. M06/6-311+G**calculated results demonstrate that the transition state, **TS-a**, is 51.81, 58.92 and 59.02 kcal mol^{-1} higher in electronic energy relative to the initial tautomer in the gas phase and in the presence of DMF and H_2O as solvents, respectively.

In the second step of tautomerization reaction, C3-H bond is broken followed by transition state, **TS-b**, to generate N2-H σ-bond (M06/6-311+G**calculated bond distance is 1.011 Å) in the final product. It should be stated that M06/6-311+G**calculated electronic energy of transition state, **TS-b**, is 44.51, 51.61 and 51.73 kcal mol^{-1} higher relative to **tautomer-a** in the gas phase, DMF and H_2O solutions, respectively. In another word, energy barrier of **TS-b** in the gas phase is 22.35 kcal mol^{-1} while in H_2O and DMF solution phases are 23.29 and 23.30 kcal mol^{-1}, respectively that are approximately the same.

It should be noted that the imaginary frequencies of

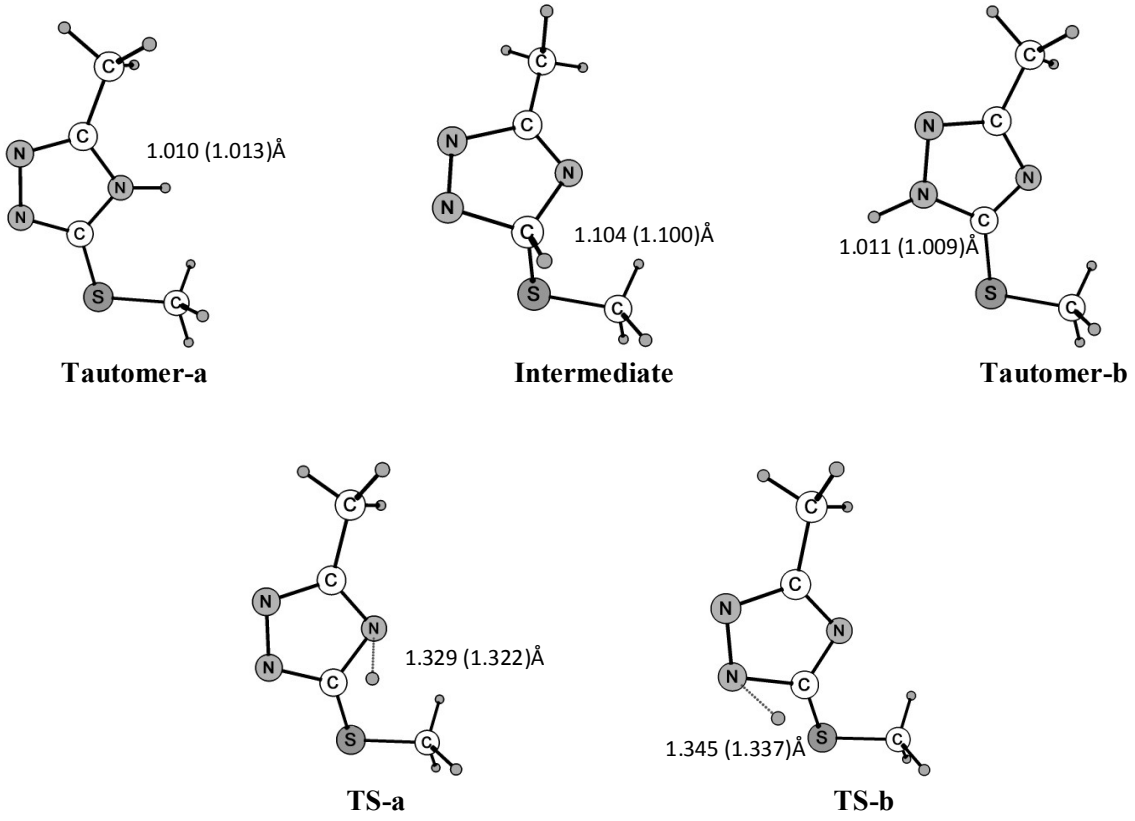

Fig. 2. The optimized geometry of tautomers, intermediate and transition states, calculated at M06/6-311+G** level of theory. Note that the reported bond distance values in the parenthesis are corresponded to B3LYP/6-311+G** calculations.

Table 1. Thermochemistry of Aforementioned Tautomeric Reaction Calculated at B3LYP/6-311+G** and M06/6-311+G** Levels of Theory in the Gas and Two Solution Phases. $\Delta E_{e,r}$ is the Reaction Electronic Energy Change, $\Delta E_{0,r}$ is the Reaction Electronic Energy Change with Zero-point Energies Included, ΔH_r and ΔG_r are the Reaction Enthalpy and Free Energy Changes, Respectively. Note that B3LYP/6-311+G** Calculated Values Have Been Presented in the Parenthesis and all the Reaction Energy Values are in kcal mol^{-1}

	$\Delta E_{e,r}$	$\Delta E_{0,r}$	ΔH_r	ΔG_r
gas phase	-10.72 (-6.40)	-10.04 (-6.12)	-8.88 (-5.83)	-10.29 (-5.98)
solution phase				
DMF	-5.06 (-3.56)	-4.52 (-3.28)	-3.98 (-2.64)	-4.91 (-3.48)
H_2O	-4.93 (-2.82)	-4.40 (-2.61)	-3.87 (-2.03)	-4.88 (-2.77)

transition states correspond to the increase of N4-H and N2-H in **TS-a** and **TS-b** species, respectively, have been obtained 1559.98 cm^{-1} and 1452 cm^{-1}.

In Figs. 3 and 4, we display schematically the relative electronic energy diagrams of the tautomerism pathway in the gas and solution phases, respectively. In these figures, we presentthe electronic energy diagrams obtained at both B3LYP/6-311+G** and M06/6-311+G** levels of theory. The following two facts can be deduced from the comparative survey of Figs. 3 and 4, i) based on both B3LYP/6-311+G** and M06/6-311+G**calculation results, the energy barrier of **TS-a** in the gas phase increases in the solution medium while the energy barrier of **TS-b** in the gas and solution phases have the same values and ii) the employment of two solvents, DMF and H_2O, leads to the near calculated results mechanistically in the overall reaction pathway. In Fig. 5, we also present comparatively the potential energy profile of tautomeric mechanism obtained via IRC calculations at B3LYP/6-311+G** and M06/6-311+G** levels of theory in the gas phase.

QTAIM Interpretations of Tautomerism

Another objective of this research is to investigate the electronic features of aforementioned tautomeric

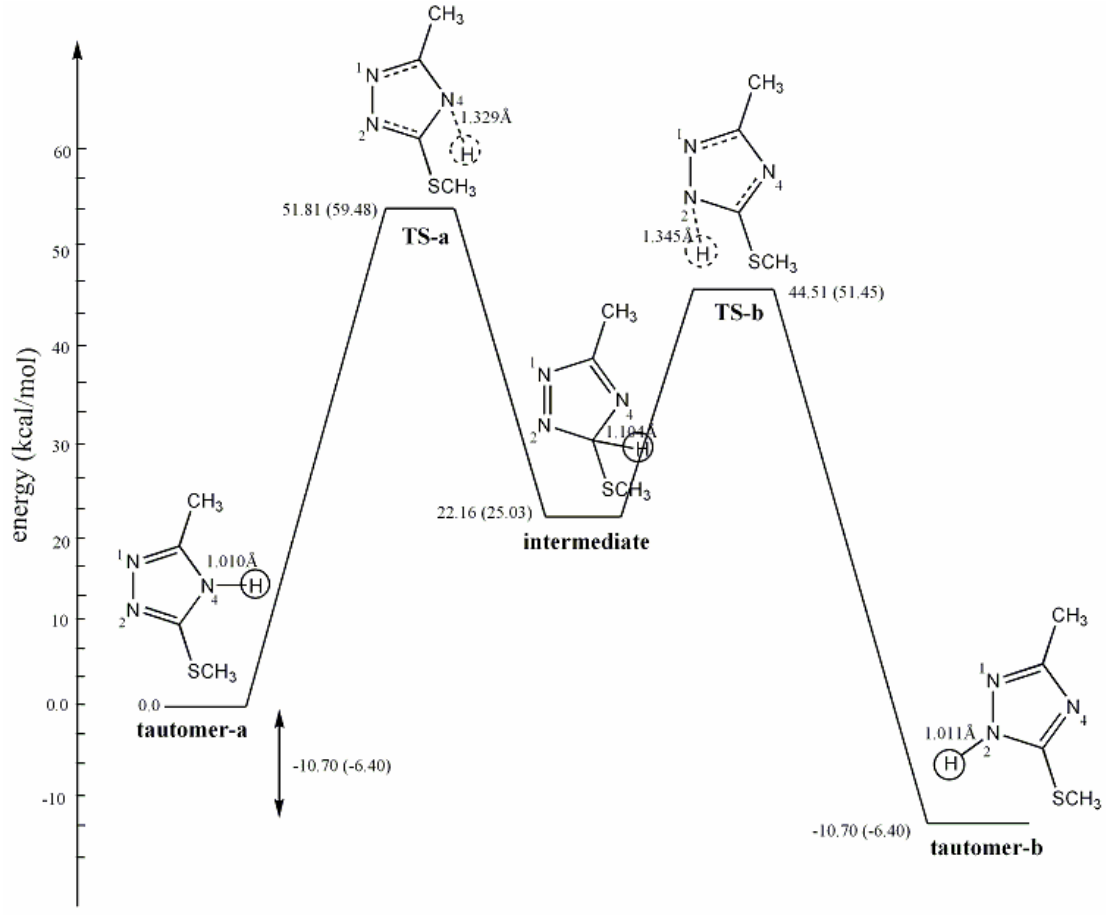

Fig. 3. The relative electronic energy diagram for the unimolecular tautomerization of 5-methyl-3-methylthio-1,2,4-triazole in the gas phase calculated at M06/6-311+G** level of theory. Note that the corresponding B3LYP/6-311+G** calculated values have been reported in the parenthesis.

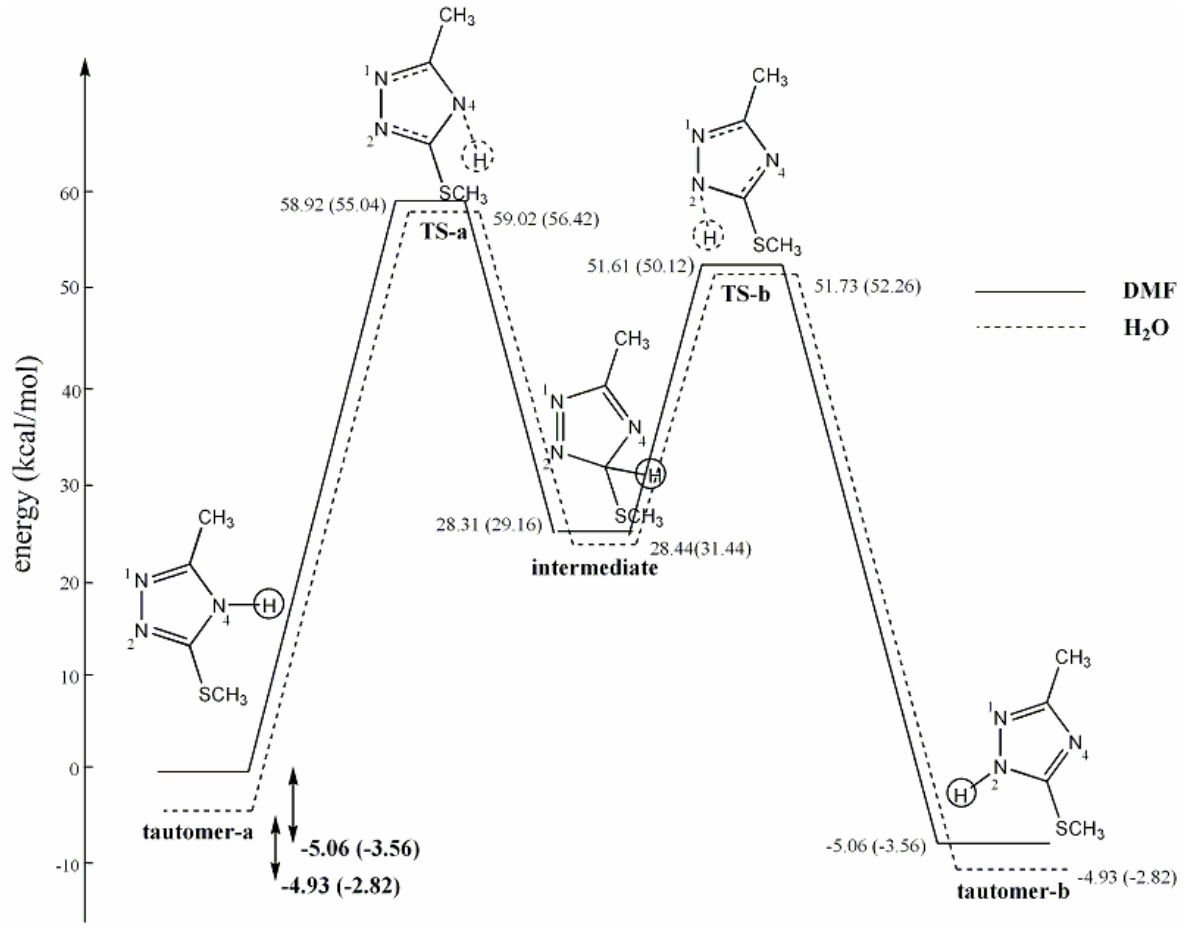

Fig. 4. The relative electronic energy diagram for the unimolecular tautomerization of 5-methyl-3-methylthio-1,2,4-triazole in the presence of H_2O (dashed line ----) and DMF (solid line —) as solvents by inclusion of solvation model, calculated at M06/6-311+G** level of theory. Note that the corresponding B3LYP/6-311+G** calculated values have been reported in the parenthesis.

mechanism *via* topological QTAIM analysis of bonding interactions in terms of electron density and its derivatives [24]. The Laplacian of the electronic charge density, $\nabla^2\rho(r)$, indicates whether the electron density is locally concentrated ($\nabla^2\rho(r) < 0$) or depleted ($\nabla^2\rho(r) > 0$). Accordingly, a negative value of $\nabla^2\rho(r)$ at BCP is related to the covalent character of a bond, while $\nabla^2\rho(r) > 0$ implies "closed-shell-type" interaction as found in ionic bonds, hydrogen bonds, and van der Waals molecules. The electronic energy density, H(*r*), at the BCP has also been defined as H(*r*) = G(*r*) + V(*r*), where G(*r*) and V(*r*) correspond to kinetic and potential energy densities, respectively [25-27]. The sign of H(*r*) determines whether accumulation of charge at a given point, r, is stabilized, H(*r*) < 0, or destabilized, H(*r*) > 0.

In Table 2, we report the calculated values of electron density, its Laplacian, kinetic and potential energy densities and also the total electronic energy density at some selected BCPs of tautomers, intermediate and transition states. In Fig. 6, we illustrat AIM representation of tautomers, intermediate and transition states which is the collection of all critical points of electron density and their associated

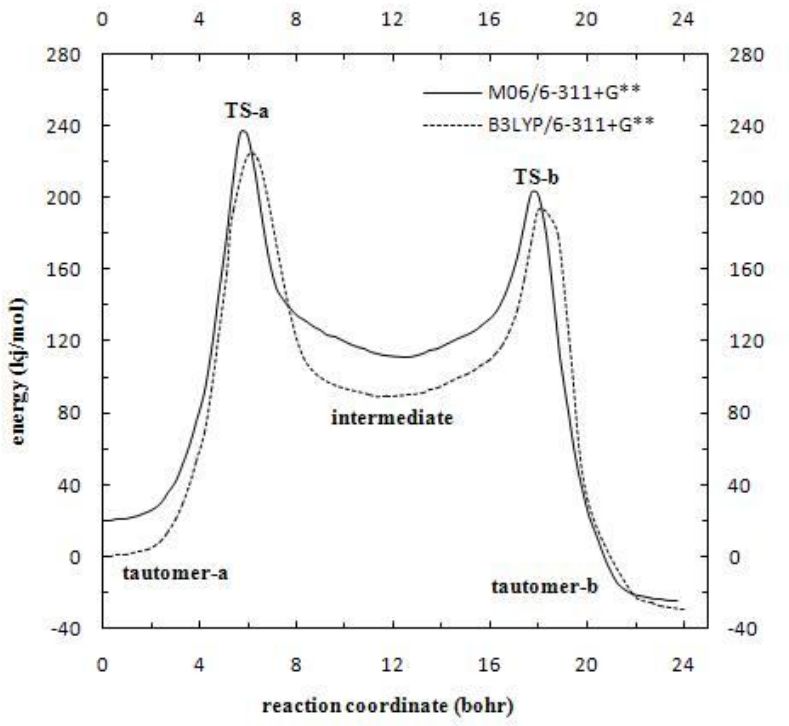

Fig. 5. The potential energy profile of tautomeric mechanism obtained *via* IRC calculations in the gas phase at B3LYP/6-311+G** (dashed line ----) and M06/6-311+G** (solid line —) levels of theory.

Table 2. Mathematical Properties of BCPs Associated to some Selected Bonds in the Tautomers, Transition States and Intermediate. The Properties have been Obtained *via* QTAIM Analysis on the M06/6-311+G** Calculated Wave Function of Electron Density. Note that Numbering of Atoms is in Accordance with Fig.1

	ρ(r)	$\nabla^2\rho$(r)	V(r)	G(*r*	H(*r*)
Tautomer-a (N4-H)	0.325	-1.615	-0.491	0.043	-0.447
TS-a (C3-H)	0.174	-0.153	-0.170	0.066	-0.104
Intermediate (C3-H)	0.266	-0.883	-0.292	0.035	-0.256
TS-b (C3-H)	0.177	-0.179	-0.171	0.063	-0.107
Tautomer-b (N2-H)	0.328	-1.659	-0.495	0.040	-0.455

bond paths. We remind that our focus of QTAIM analysis is on the M06/6-311+G** calculated wave function of electron density obtained for the optimized structures of tautomers, intermediate and transition states. The reported results in Table 2, clearly show the following facts: i) the negative values of $\nabla^2\rho$(r) and also H(*r*) at all selected BCPs determine the amassing charge in the bonded region and consequently imply the presence of covalent bond critical points, ii) a comparative survey of topological electronic indices between transition states with their corresponding

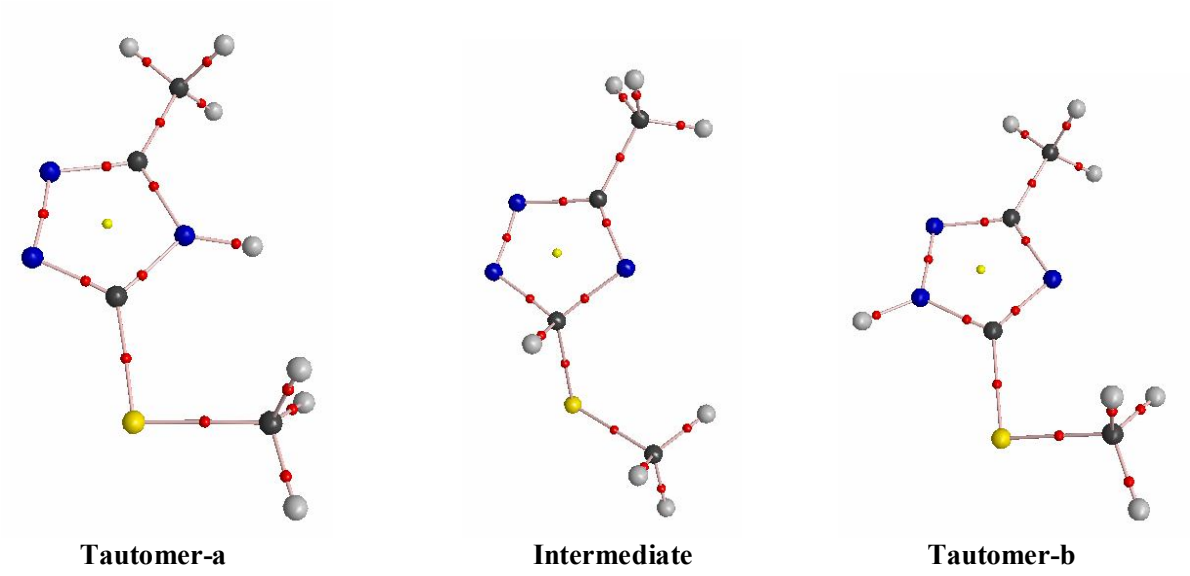

Fig. 6. Complete molecular graphs (MGs) of tautomers, intermediate and transition states obtained by QTAIM analysis of M06/6-311+G** electron density. Bond Critical Points: red circles; Ring Critical Points: yellow circles; Bond Paths: pink lines.

Table 3. QTAIM Calculated Values of Ellipticity at Two Selected BCPs of Tautomers and Intermediate. Note that Numbering of Atoms is in Accordance with Fig.1

Ellipticity	**Tautomer-a**	**Intermediate**	**Tautomer-b**
N2-C3	0.345	0.048	0.210
C3-N4	0.166	0.022	0.229

tautomers demonstrates that there is no bond critical point at N4-H and N2-H in **TS-a** and **TS-b**, respectively. And iii) the values of $\rho(r)$ for C3-H bond in **TS-a** and **TS-b** are lower than those in the intermediate species correlated with the fact that C3-H bond has been elongated and thus weakened in the transition states.

Another interesting aspect of QTAIM calculations can be derived from the analysis of ellipticity values, ε. Ellipticity is a measure of the π-character of the bonding up to the limit of the double bond for which the ellipticity reaches to a maximum. On going from a double to the triple or single bonds, the trend is reversed and the ellipticity decreases till to vanish, $\varepsilon \approx 0$, regarded as the cylindrical symmetry. In Table 3, we report the calculated elliptic ties for N2-C3 and C3-N4 bonds in the tautomers and intermediate. On the basis of these values, N2-C3 bond has a more double bond character than that of C3-N4 bond in **tautomer-a,** while this behavior shows a reverse trend in **tautomer-b**. Moreover, as we expected the obtained ellipticity values confirm the σ-character for N2-C3 and C3-N4 bonds (with the small $\varepsilon << 0.1$ values) in the intermediate species.

CONCLUSIONS

As a primary purpose, we have surveyed and illustrated the tautomeric reaction pathway of 5-methyl-3-methylthio-1,2,4-triazole in the gas and solution phases from the

mechanistical and thermodynamical points of view. The B3LYP/6-311+G** and M06/6-311+G** calculated results revealed the following two facts: i) the tautomeric form of 5-methyl-3-methylthio-1,2,4-triazole with a tautomeric-proton connected to pyrole-like nitrogen atom possess the larger thermodynamical stabilization energy in the gas and solution phases and ii) thermodynamic feasibility of tautomerism decreases in the solution medium compared with the gas phase while there is a little thermodynamical distinction between using two solvents. Overall, the stringent analysis of the calculated thermodynamical and mechanistical results of the proposed 1,3-proton transfer pathway reveals that the production of **tautomer-b** is more favorable thermodynamically than that of **tautomer-a** while the energy barrier for the conversion of **tautomer-a** to **tautomer-b** is relatively high.

Another important aspect of aforementioned tautomerism, deduced from our QTAIM calculations, is the electronic feature. Topological analysis of electron density and its laplacian confirms that lengthening of C3-H bond in **TS-a** and **TS-b** species is in correlation with the ρ(r) calculated values of C3-H bond critical point. Finally, the calculated elliptic ties indicate the π-character of N2-C3 and C3-N4 bonds in **tautomer-a** and **tautomer-b**, respectively, while the aforesaid N2-C3 and C3-N4 bonds in the intermediate have been considered as σ-bond type. In overall we can claim that all of our QTAIM interpretations are in agreement with the proposed tautomeric reaction path.

ACKNOWLEDGMENTS

The author gratefully acknowledges the partial financial support received from the research council of Alzahra University. The author is also grateful to Prof. Majid M. Heravi for his helpful suggestions.

REFERENCES

[1] A.R. Katritzky, C.A. Ramsden, J.A. Joule, V.V. Zhdankin, Handbook of Heterocyclic Chemistry, 3rd ed., Elsevier, Oxford, 2010.

[2] A.R. Katritzky, C.A. Ramsden, E.F.V. Scriven, R.J.K. Taylor, Comprehensive Heterocyclic Chemistry-III, Elsevier, Oxford, 2008.

[3] M.D. Mullican, M.W. Wilson, D.T. Connor, C.R. Kostlan, D.J. Schrier, R.D. Dyer, J. Med. Chem. 36 (1993) 1090.

[4] E. Bozo, G. Szilagyi, A. Janaka, J. Arch. Pharm. 322 (1989) 583.

[5] D.H. Boschelli, D.T. Connor, D.A. Bornemeier, R.D. Dyer, J.A. Kennedy, P.J. Kuipers, G.C. Okonkwo, D.J. Schrier, C.D. Wright, J. Med. Chem. 36 (1993) 1802.

[6] R.W. Taft, F. Anvia, M. Taagepera, J. Catalfin, J. Elguero, J. Am. Chem. Soc. 108 (1986) 3237.

[7] J. Elguero, A.R. Katritzky, O.V. Denisko, Adv. Heterocycl. Chem. 76 (2000) 1.

[8] E.D. Raczynska, W. Kosinska, B. Osmiatowski, R. Gawinecki, Chem. Rev. 105 (2005) 3561.

[9] M.M. Heravi, A. Kivanloo, M. Rahimzadeh, M. Bakavoli, M. Ghassemzadeh, B. Neumüller, Tetrahedron Lett. 46 (2005) 1607.

[10] M.M. Heravi, H.R. Khademalfoghara, M.M. Sadeghi, Sh. Khaleghi, M. Ghassemzadeh, Phosphorus, Sulfur Silicon Relat. Elem. 181 (2006) 377.

[11] M.M. Heravi, A. Kivanloo, M. Rahimzadeh, M. Bakavoli, M. Ghassemzadeh, Phosphorus, Sulfur, Silicon Relat. Elem. 177 (2002) 2491.

[12] T. Hosseinnejad, M.M. Heravi, R. Firouzi, J. Mol. Model. 19 (2013) 951.

[13] A.D. Becke, J. Chem. Phys. 98 (1993) 1372.

[14] C. Lee, W. Yang, R.G. Parr, Phys. Rev. B. 37 (1988) 785.

[15] D.G. Truhlar, Y. Zhao, Theor. Chem. Account. 120 (2008) 215.

[16] V. Barone, M. Cossi, M. J. Phys. Chem. A 102 (1998) 1995.

[17] M.M. Heravi, S. Sadjadi, Tetrahedron 65 (2009) 7761.

[18] C. Amatore, E. Carré, A. Jutand, A. Acta Chem. Scand. 52 (1998) 100.

[19] R.F.W. Bader, Atoms in Molecules: a Quantum Theory, Oxford University Press, Oxford, 1990.

[20] M.W. Schmidt, K.K. Baldridge, J.A. Boatz, S.T. Elbert, M.S. Gordon, J.H. Jensen, S. Koseki, N. Matsunaga, K.A. Nguyen, S.J. Su, T.L. Windus, M. Dupuis, J.A. Montgomery, J. Comput. Chem. 14 (1993) 1347.

[21] C. Gonzales, H.B. Schlegel, J. Chem. Phys. 90 (1989) 2154.

[22] C. Gonzales, H.B. Schlegel, J. Chem. Phys. 95 (1991) 5853.
[23] R.F.W. Bader, AIM2000 Program, ver 2.0, Hamilton, McMaster University, 2000.
[24] R.F.W. Bader, Chem. Rev. 91 (1991) 893.
[25] D. Cremer, E. Kraka, Angew. Chem. 23 (1984) 627.
[26] K. Wiberg, Tetrahedron 24 (1968) 1093.
[27] S. Jenkins, I. Morrison, Chem. Phys. Lett. 317 (2000) 97.